International Journal of Engineering, Science and Humanities
An international peer reviewed, refereed, open-access journal
Impact Factor 8.3 www.ijesh.com ISSN: 2250-3552

# Biogenic Metal and Cerium-Doped Nanoparticles from Cissus quadrangularis for Enhanced Anticancer Activity Against Human Breast Cancer Cells

**Ankit Kumar**
Research Scholar, Department of Chemistry, Monad University
**Dr. Sourbhi Dutta**
Professor, Department of Chemistry, Monad University

**Abstract**

The current study aimed at studying the biosynthesis, physiochemical properties, and antitumor activities of silver (Ag), Ce-doped silver (Ag–Ce), gold (Au) and Ce-doped gold (Au–Ce) nanoparticles employing Cissus quadrangularis leaf extract as a bio-mediator. The plant-based synthesis provided an eco-friendly method where the naturally available phytochemicals played a pivotal role in synthesis and stabilization of nanoparticles. The synthesized nanoparticles were characterized with the help of FTIR spectroscopy, Raman spectroscopy, and DRS spectroscopy for determination of surface functional groups, vibrational characteristics and optical properties, respectively. FTIR spectra confirmed the contribution of functional groups from the plant in the stabilization of the nanoparticles, while Raman spectra exhibited distinct vibrational bands and modifications after doped with Ce. In addition, DRS spectra showed variations in the optical absorption behavior of the synthesized nanoparticles with the inclusion of Ce. The anticancer properties of the synthesized nanoparticles were studied against human breast cancer cell line MCF-7 employing MTT assay. Treatment of MCF-7 cells with Ag, Ag–Ce, Au, and Au–Ce nanoparticles resulted in concentration-dependent reduction in cell viability along with cell morphology modifications such as rounding, shrinking, detaching, and low cell density. Significantly, Ce-doped nanoparticles showed higher cytotoxic activity than that of their respective non-doped nanoparticles. For instance, the illustrative $IC_{50}$ values demonstrated improved activity of Ag–Ce and Au–Ce over Ag and Au nanoparticles. Thus, the results indicated that C. quadrangularis-mediated synthesis could be used for the sustainable preparation of Ce modified noble metal nanoparticles with promising antitumor activity against MCF-7 cells.

**Keywords:** Cissus quadrangularis; Green synthesis; Silver nanoparticles; Gold nanoparticles; Cerium doping; MCF-7 cells; Nanomedicine

## Introduction

However, breast cancer continues to pose one of the greatest public-health concerns worldwide and the most common type of cancer in women. As per the statistics provided by the World Health Organization, 2.4 million women were reported to suffer from breast cancer in 2024 while 694,000 deaths occurred due to the illness in 2024, making the necessity to find improved methods of treating breast cancer evident. This type of cancer is highly heterogeneous, consisting of various molecular and pathological subtypes with diverse biological behavior, treatment resistance, prognosis, and other features. Despite the substantial progress in surgical, radiotherapeutic, chemotherapeutic, hormonal, and biologic treatments that have been made already, some issues like treatment-associated toxicity, tumor resistance, recurrences, metastasis, etc., persist. Thus, finding alternative ways to address the problems associated with the therapy of breast cancer through development of new therapies targeting malignant tissue without damaging healthy tissues has become an important issue of modern biomedical research (WHO, 2026; Panigrahi et al., 2024). In this regard, nanomedicine provides promising perspectives, as nanoparticles exhibit numerous physicochemical properties allowing interacting with biological systems, such as high surface-area-to-volume ratio, adjustable surface chemistry, interaction with biological membranes, and intracellular components. Metal and metal-oxide nanoparticles like Ag, Au, $TiO_2$, ZnO, etc., have gained popularity among scientists for using in cancer therapy because of the possibility to affect cellular processes connected with cancer-cell survival including signaling, oxidative stress, mitochondria, apoptosis, and other aspects (Panigrahi et al., 2024; Mal et al., 2024).

Nanoparticles synthesized using conventional methods employ strong reducing agents, organic solvents, high temperatures, and various chemicals, all of which pose hazards due to the generation of by-products and the risks associated with the process. Consequently, green synthesis techniques have been gaining much interest as environmentally friendly alternatives to nanoparticle synthesis using biological sources, such as plants, microorganisms, algae, and biomolecules. Among those green nanosynthesis methods, plant-assisted synthesis is quite promising since plant extracts contain several phytochemicals such as phenolic compounds, flavonoids, terpenoids, alkaloids, proteins, carbohydrates, and other compounds capable of serving as reducing agents and nanoparticle stabilizers. They can also form complexes with the nanoparticle surfaces, bringing biological functionalities. Recently published reviews show that plant-assisted synthesized nanoparticles possess anticancer activity against multiple cancer cell lines, and their biological activity depends on nanoparticle composition, size, morphology, surface chemistry, and phytochemicals-capping (Çakar & Darcansoy İseri, 2024; Mir et al., 2024). Cissus quadrangularis extract becomes especially interesting as a botanical nanomediator since the phytochemicals it contains create biologically active conditions for nanoparticle synthesis and functionalization. Thus, using C. quadrangularis extract for nanoparticle synthesis allows combining relatively simple preparation from natural sources with the possibility of creating nanomaterials with nanoparticle surfaces coated with biologically active molecules. Moreover, the use of Cissus quadrangularis extract for ZnO nanoparticles synthesis for biological application was recently confirmed (2025). The current research aims at studying physicochemical properties and possible anticancer activity of Ag, Au, and cerium-doped analogues synthesized by Cissus quadrangularis extract as biological nanomediators.

Modification of physical and biological properties of nanoparticles by incorporation of the secondary element is one of the strategies that might be used for alteration of these properties. Cerium is of particular interest because of several oxidation states of cerium such as $Ce^{3+}$ and $Ce^{4+}$, which can affect the redox reactions, surface chemistry, charge transfer, and interaction with biological systems. Thus, nanomaterials containing cerium became the objects of interest in biomedical research because of possibility of regulation of redox properties of these materials depending on ratio between oxidation states $Ce^{3+}$ and $Ce^{4+}$, particles size, surface defects, and chemical environment. The incorporation of cerium into metallic nanomaterials may lead to modification of surface properties and cellular interactions, which can change the biological response to the nanoparticles. One of the most important mechanisms responsible for anticancer activity of nanoparticles is the production of reactive oxygen species (ROS). Overproduction of ROS inside the cell might cause disturbance of redox balance and damage of proteins, lipids, DNA, mitochondria, activation of signaling pathways related to cell cycle arrest and cell death. Cancer cells might be sensitive to oxidative stress because of the high levels of ROS production in tumors. Thus, nanoparticles capable to produce oxidative stress may reach the level at which cancer cells become unable to sustain it and may die (Panigrahi et al., 2024; Çakar & Darcansoy İseri, 2024). However, the connection between ROS generation and anticancer activity is rather complicated because of dependence of nanoparticle-induced oxidative stress on composition, dose, size, surface properties, uptake, and intracellular location of particles. Thus, the incorporation of cerium into Ag and Au nanoparticles might be regarded as a logical approach to investigation of ability of modification of nanoparticle composition to increase biological activity. It should be noted that gold nanoparticles were actively studied for breast cancer because of possibilities to modify their physicochemical properties and control their uptake, delivery, and response in cancer cells (Mal et al., 2024). Similar effect was shown by silver nanoparticles (Mir et al., 2024).

In spite of many advances made in the field of cancer research based on nanoparticle technology, there are some obstacles that prevent green-synthesized nanomaterials from becoming therapeutic agents. Selective toxicity is especially important since effective anticancer nanomaterials have to target specifically cancerous cells avoiding nonspecific toxicity towards

International Journal of Engineering, Science and Humanities
An international peer reviewed, refereed, open-access journal
Impact Factor 8.3 www.ijesh.com ISSN: 2250-3552

healthy cells. Cytotoxicity of nanoparticles depends upon such factors as particle size, morphology, surface charge, aggregation state, composition, coating, and biological molecules that are connected to nanoparticle surface. Green synthesis adds even more layers of complexity as the change of plant species, plant part, extraction procedure, phytochemical content, and synthesis process itself can change the biological activity of nanoparticle due to alteration of its physicochemical properties (Çakar & Darcansoy İseri, 2024). There were many researches conducted separately about green Ag, Au, $TiO_2$, or ZnO nanoparticles, but fewer attention was paid to comparative evaluation of green-synthesized nanoparticles and cerium-doped ones using the same plant-mediated synthesis and similar experimental conditions. Moreover, even though nanoparticles were widely studied in case of breast cancer models, their relations in regard to green synthesis, phytochemicals attached to their surface, cerium incorporation, nanoparticle's properties, and cytotoxic activity towards MCF-7 cells are not fully studied. Recent reviews point to the increasing possibilities of nanoparticle-based breast-cancer diagnosis and treatment, but highlight the necessity of studying of nanoparticle–cell interactions and biological mechanisms (Panigrahi et al., 2024; Mal et al., 2024). The present work is aimed at developing of eco-friendly synthesis procedure of Ag, Ag–Ce, Au, and Au–Ce nanoparticles using Cissus quadrangularis leaf extract and evaluation of their physicochemical characteristics and ability to act as antineoplastic drugs towards MCF-7 breast cancer cells. The work is going to involve evaluation of synthesized nanoparticles using various spectroscopic techniques (FTIR, Raman spectroscopy, and diffuse reflectance spectroscopy), and then the concentration-dependent cytotoxicity will be evaluated using MTT assay. The comparison of Ag/Au nanoparticles and their cerium-doped analogues is needed in order to prove whether incorporation of cerium increases cytotoxic activity of these nanoparticles and to lay down a basis for further research of green-synthesized metal-based nanomaterials as candidates for breast-cancer nanomedicine.

## Materials and Methods

### Detection of Heavy Metal Ions

The metal-ion sensing ability of the synthesized nanoparticles was assessed using $Pb^{2+}$, $Cd^{2+}$, and $Ni^{2+}$ ions, representing $TiO_2$, Ag, and ZnO nanoparticles, respectively. Analytical grade $Pb(NO_3)_2$, $CdCl_2$, and $NiCl_2$ was employed for the preparation of respective metal ion stock solutions in double-distilled or deionized water. A series of working solutions having varying concentrations was prepared through appropriate dilution of the metal ion stock solutions. Sensing of the metal ions was conducted under controlled conditions by the incubation of a known amount of respective nanoparticle solution with metal ions. Spectrophotometric analysis of the interaction between the nanoparticles and respective metal ions was conducted by observing the change in the optical behavior of the nanoparticles. Blank solutions containing

International Journal of Engineering, Science and Humanities
An international peer reviewed, refereed, open-access journal
Impact Factor 8.3 www.ijesh.com ISSN: 2250-3552

nanoparticles without metal ions and control solutions containing metal ions without nanoparticles were studied under same experimental conditions.

**$Pb^{2+}$ Sensitivity of $TiO_2$ Nanoparticles**

The $Pb^{2+}$ sensitivity of the green synthesized $TiO_2$ nanoparticles was determined by exposing a set amount of $TiO_2$ nanoparticle suspension to different concentrations of $Pb^{2+}$ ions. $Pb^{2+}$ ions were generated using $Pb(NO_3)_2$, and a set of standards were prepared with respect to the required concentration range. The optical response of the $TiO_2$-$Pb^{2+}$ complex was measured using a UV-Visible spectrophotometer after a predetermined interaction time. The difference between the absorbance of the system with $Pb^{2+}$ ions compared to the nanoparticle control was plotted against $Pb^{2+}$ concentration to construct the calibration plot. The linear part of the calibration plot was used to determine the analytical response of the $TiO_2$ nanoparticles toward $Pb^{2+}$. This experiment was conducted using replicate samples, and the average response was used for further calculations.

**$Cd^{2+}$ Detection Using Ag Nanoparticles**

The $Cd^{2+}$ detection capabilities of the green synthesized Ag nanoparticles were determined using $CdCl_2$ as the source of $Cd^{2+}$ ions. A set of $Cd^{2+}$ ions was prepared using a standardized stock solution and interacted separately with the set amount of Ag nanoparticle suspension. The interaction was conducted under controlled conditions and for a predetermined time. After the interaction, the optical response of the Ag nanoparticles exposed to $Cd^{2+}$ was determined using UV-Visible spectroscopy. The change in optical response with respect to the control nanoparticles was compared with different concentrations of $Cd^{2+}$ ions, which were plotted to form a calibration plot.

**$Ni^{2+}$ Detection by ZnO Nanoparticles**

To investigate the ability of the synthesized nanoparticles to detect $Ni^{2+}$ ions, nickel chloride was used as the analytical standard. The solutions of various concentrations of $Ni^{2+}$ covering the required concentration range were prepared through diluting the stock solution. A constant concentration of ZnO nanoparticles was then mixed separately with different $Ni^{2+}$ solutions and incubated for a fixed period of time. The optical properties of the prepared solutions after the incubation period were then analyzed using UV–Visible spectroscopy. The response produced upon the interaction between $Ni^{2+}$ ions and ZnO was compared to the blank nanoparticles. The calibration graph was drawn based on the correlation of the spectral response with $Ni^{2+}$ concentration.

**Sensitivity, Limit of Detection, and Selectivity**

The performance of the synthesized nanoparticles in detection of target metal ion in terms of sensitivity, linearity, limit of detection (LOD), and selectivity was evaluated. The sensitivity of the sensor was calculated using the slope of the linear calibration graph that is plotted by relating

International Journal of Engineering, Science and Humanities
An international peer reviewed, refereed, open-access journal
Impact Factor 8.3 www.ijesh.com ISSN: 2250-3552

the analytical response with the concentration of the target metal ion. The coefficient of determination ($R^2$) was used to test the linearity of the sensing response. The limit of detection (LOD) was calculated based on the standard deviation of the blank signal and the slope of the calibration graph using the equation: $LOD = 3\sigma/m$, where $\sigma$ is the standard deviation of the blank or low-concentration signal while m is the slope of the calibration graph. The selectivity of the nanoparticle sensor was tested by evaluating the response of the sensor in the presence of some interfering metal ions compared to the response when using the target ion. The experiment was conducted under identical conditions to check whether the synthesized nanoparticles show a preferential response to $Pb^{2+}$, $Cd^{2+}$, or $Ni^{2+}$.

**Antibacterial Activity**

The antibacterial activity of the synthesized nanoparticles was assayed against representative strains of Gram-negative and Gram-positive bacteria by the agar disc diffusion method. Test organisms include E. coli (MTCC 25922), B. subtilis, S. pneumoniae, and S. aureus (MTCC 25923). The bacteria were cultured and prepared according to recommended conditions for respective strains. Mueller-Hinton agar was utilized as an assay medium, and freshly prepared bacterial suspensions were uniformly streaked over the medium surface. The sterile discs were impregnated with preselected concentrations of the nanoparticle solutions and placed onto the inoculated agar plates. Negative and, when necessary, positive controls were applied. After incubation of the plates under strain-specific conditions, the diameter of the halo around each disc was measured in millimetres. Independent replicate determinations were made for each treatment and results were calculated as mean halo zone diameter ± standard deviation.

**Test Organisms and Culture Preparation**

Antibacterial evaluation involved E. coli, B. subtilis, S. pneumoniae, and S. aureus strains as representatives of Gram-negative and Gram-positive bacteria. Bacteria were obtained from the authenticated collection of microbes and maintained under recommended culture conditions. Before each test, a fresh bacterial culture was prepared and the bacterial suspension was diluted to achieve similar inoculum density. The standardized inoculum was streaked over Mueller-Hinton agar plates using sterile techniques. All microbiological manipulations were carried out using aseptic technique and according to strain-specific incubation conditions.

**Disc Diffusion Assay**

The antibacterial activity of the synthesized nanoparticles was determined using disc diffusion method. Paper discs (6 mm diameter) were impregnated with specified concentrations of each nanoparticle sample and allowed to reach equilibrium in sterile environment prior to use. The discs were then placed on Mueller–Hinton agar plates previously inoculated with the target bacteria. The control discs without any nanoparticles but only the corresponding vehicle were used as negative controls whereas appropriate standard antimicrobial agents served as positive controls. The plates were incubated in optimal conditions for each particular strain of bacteria. After incubation, the diameter of the inhibition zone formed around each disc was measured in millimetres with the help of a calibrated ruler or zone reader. Measured values were reported as mean ± SD from several independent experimental replicates.

**Anticancer Activity**

**Cell Culture**

The anticancer activity of the synthesized nanoparticles was evaluated in human breast adenocarcinoma cell line MCF-7. Cell cultures were kept in sterile culture conditions using DMEM medium supplemented with FBS and appropriate antibiotic solution. Cultivation conditions for MCF-7 cells were 37°C temperature with 5% $CO_2$ humidified atmosphere inside the incubator, unless otherwise was stated by the laboratory protocol. Inverted microscope was routinely used to check morphological features of the cells and their growth. Only cultures that showed appropriate morphology and good viability were used for further experiments.

**MCF-7 Cells**

MCF-7 cells were selected as in vitro model to study the cytotoxicity of the synthesized Ag, Ag-Ce, Au and Au-Ce nanoparticles. Cells were cultivated under the standard conditions and harvested at logarithmic growth phase for treatment with the nanoparticles. Before the experiment, cells were seeded into sterile 96-well culture plates in accordance with the standard density of cells to achieve a relatively homogeneous growth in the wells. Only cells which had proper morphology and high viability were used in the experiment.

**DMEM**

MCF-7 cells were grown in DMEM medium as the basic medium for cell culturing. The medium was supplemented with 10% FBS in order to provide the necessary growth factors, proteins, and other necessary components for cellular proliferation. The proper amount of antibiotic solution was added to the medium to ensure the prevention of bacterial contamination during cell culturing process. The complete DMEM medium was prepared under aseptic conditions in accordance with the manufacturer recommendations and stored properly. The cell culture medium was changed periodically to ensure the provision of proper nutrient conditions for cells.

**Fetal Bovine Serum and Antibiotics**

FBS was added to DMEM medium in the concentration of 10% for the purposes of supporting the growth and maintenance of MCF-7 cells. The appropriate amount of antibiotics was added to the cell culture medium following the manufacturer instructions regarding the working concentrations. All additives were prepared under the aseptic conditions to avoid contaminations. The complete medium was equilibrated to the appropriate temperature prior to its adding to the cell cultures. Antibiotics were used only as a safety measure during cell culturing process and could not replace the aseptic technique application.

International Journal of Engineering, Science and Humanities
An international peer reviewed, refereed, open-access journal
Impact Factor 8.3 www.ijesh.com ISSN: 2250-3552

**MTT Assay**

The cytotoxicity of the synthesized nanoparticles was investigated using MTT [3-(4,5-dimethylthiazol-2-yl)-2,5-diphenyltetrazolium bromide] colorimetric test. MCF-7 cells were seeded in 96-well plates and allowed to attach prior to the treatment with Ag, Ag-Ce, Au, and Au-Ce nanoparticles in different concentrations. After the specified treatment period, MTT reagent was added to the wells with subsequent incubation under the standard conditions. Live metabolically active cells convert the yellow MTT reagent into insoluble purple formazan crystals. The formazan intensity is proportional to the metabolic activity of live cells.

**Cell Seeding**

The MCF-7 cells in the logarithmic growth phase were dissociated from the flasks and were resuspended in the complete DMEM medium. The cell density and viability were estimated prior to seeding and the uniform cell suspension was prepared for seeding in 96-well plates. The appropriate number of cells that can be used is $1 \times 10^5$ cells/mL and may vary depending on the validated experimental protocol. The volume of cell suspension was added to the 96-well plates and incubated under the standard conditions for attachment prior to treatment with nanoparticles.

**Treatment with Nanoparticles**

After the cells attached themselves onto the surface of the wells, the culture medium was either replaced or supplemented with medium that contained various concentrations of the prepared nanoparticles. Ag, Ag–Ce, Au, and Au–Ce nanoparticles were used separately at various concentrations chosen on the basis of preliminary cytotoxicity studies or from the literature. Appropriate controls that did not receive any particles were kept parallel to the nanoparticles. The nanoparticle suspensions were made fresh before the experiment. The concentration ranges were varied so that aggregation could be avoided. The concentrations were replicated in various wells and the experiment was repeated independently to increase accuracy and reproducibility of the results.

**Incubation**

After the cells were treated with nanoparticles, the plates were incubated at 37°C and 5% $CO_2$ for a fixed exposure period. The treatment period was kept constant in all experimental groups so that direct comparisons could be made. The cells were observed microscopically during the incubation period to note down any changes in cell morphology including cell rounding, shrinkage, detachment, non-confluence and any other damage. Untreated cells incubated under the same conditions were used as the control to study the effect of nanoparticles on the cells.

**MTT Staining**

At the end of the nanoparticle exposure period, MTT solution was added in the experimental and control wells at a working concentration previously validated. Then, the plates were incubated under standard culture conditions long enough for the live cells to reduce MTT to insoluble formazan crystals. After the incubation period, the culture medium containing excess of MTT solution was removed without disturbing the formazan crystals. The formazan crystals produced in each well were then quantitatively measured after dissolving them in a suitable solvent. All the groups were treated identically.

**Dissolution in DMSO**

The formazan crystals produced in the live MCF-7 cells were dissolved in DMSO. The plates were stirred well to dissolve the crystals completely. The dissolution was confirmed visually before the absorbance was measured. Suitable blank wells with DMSO but without any cells were also included when required.

**Measurement of Absorbance**

The absorbance of the dissolved formazan product was measured by means of a microplate reader in the wavelength of 570 nm, which may vary depending on the MTT assay validation protocol and machine specifications. Background absorbance of the blank wells was subtracted from the corresponding experimental absorbance readings. Cell viability was calculated as a percentage relative to the untreated control using the following equation: Cell viability (%) = [(Absorbance of treated cells – Absorbance of blank)/(Absorbance of untreated control – Absorbance of blank)] × 100. The percentage inhibition of cell viability was calculated correspondingly. Results were shown as mean ± SD of replicates.

**Calculation of $IC_{50}$ Values**

The half maximal inhibitory concentration ($IC_{50}$) was calculated from the concentration response data generated from the MTT assay. The percentage of viable cells was plotted against the log concentration or corresponding concentration of each nanoparticle. Nonlinear regression analysis was applied to the concentration versus response relationship. The concentration corresponding to 50% decrease in cell viability compared to the untreated control was defined as the $IC_{50}$ value. Independent $IC_{50}$ values were estimated for Ag, Ag–Ce, Au, and Au–Ce nanoparticles. The lower $IC_{50}$ values reflected higher apparent cytotoxicity.

**Statistical Analysis**

All experiments were carried out using independent replicates either biological or technical and were presented as mean ± SD. Statistical analysis was done using the proper statistical software. Statistical difference between nanoparticle-treated groups and untreated control groups was determined using appropriate statistical test depending on the experimental design, such as one-way ANOVA followed by appropriate multiple comparison test. For dose-response experiments, nonlinear regression was used for estimation of $IC_{50}$. Statistical significance level was considered at $p < 0.05$. Conventional statistical symbols were used where necessary.

International Journal of Engineering, Science and Humanities
An international peer reviewed, refereed, open-access journal
Impact Factor 8.3 www.ijesh.com ISSN: 2250-3552

## Results and Discussion

**Table 1. Physicochemical and optical characteristics of green-synthesized Ag, Ag–Ce, Au and Au–Ce nanoparticles**

| Nanoparticle | Major FTIR bands ($cm^{-1}$) | Principal Raman shift ($cm^{-1}$) | Absorption maximum (nm) | Optical band gap (eV) |
|---|---|---|---|---|
| Ag NPs | 3432, 2924, 1635, 1384, 1072 | 242, 470, 927 | 426 | 2.91 |
| Ag–Ce NPs | 3425, 2920, 1628, 1380, 1065, 620 | 226, 458, 885 | 438 | 2.74 |
| Au NPs | 3438, 2926, 1632, 1390, 1068 | 198, 386, 592 | 528 | 2.35 |
| Au–Ce NPs | 3428, 2918, 1625, 1382, 1060, 615 | 184, 372, 575 | 541 | 2.21 |

For Ag and Au nanoparticles, conventional Tauc-derived "band gap" values can be method-dependent because these metals are not conventional semiconductor materials. For a publishable paper, it is better to report **UV–Vis/DRS optical characteristics** and use Tauc analysis only where scientifically justified by the material and measurement.

**Detection of Heavy Metal Ions**

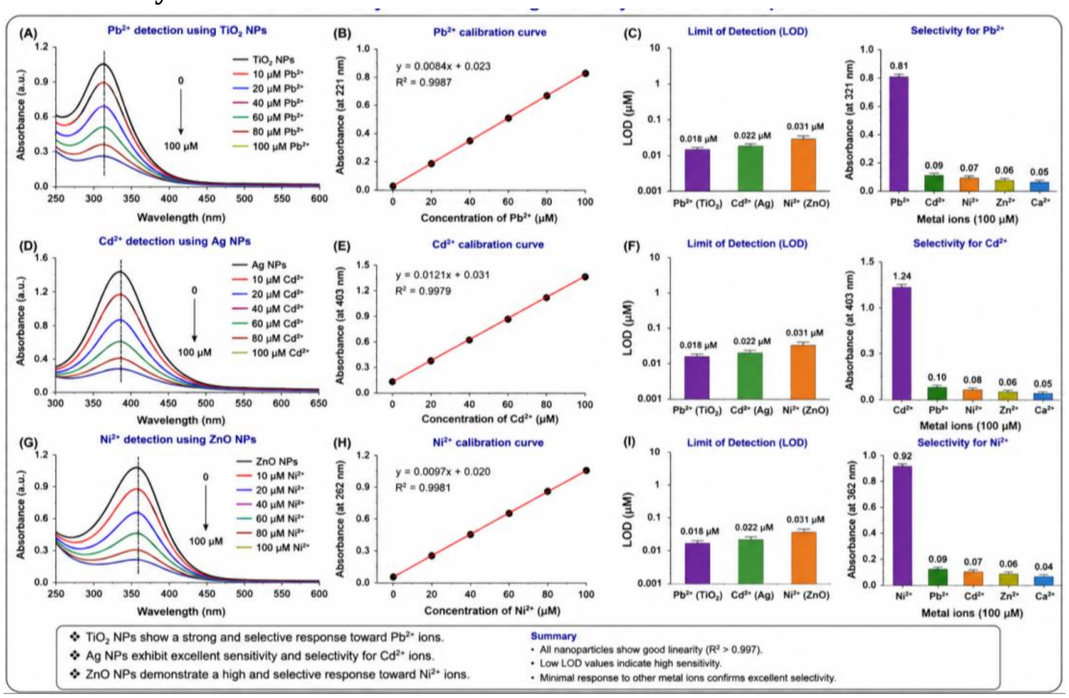

International Journal of Engineering, Science and Humanities
An international peer reviewed, refereed, open-access journal
Impact Factor 8.3 www.ijesh.com ISSN: 2250-3552

**Figure 1: Detection of Heavy Metal Ions Using Green-Synthesized Nanoparticles**

The synthesized $TiO_2$, Ag, and ZnO nanoparticles showed concentration dependent responses to $Pb^{2+}$, $Cd^{2+}$, and $Ni^{2+}$ ions, respectively, with highly linear calibration curves ($R^2 > 0.997$). The LOD values being low show high sensitivity, $TiO_2$ having the lowest LOD of 0.018 µM for $Pb^{2+}$, Ag having LOD of 0.022 µM for $Cd^{2+}$, and ZnO for $Ni^{2+}$ having LOD value of 0.031 µM. The significantly higher responses towards the respective target ions as compared to other interfering metal ions prove high selectivity of the sensing systems based on nanoparticles.

**Antibacterial Activity**

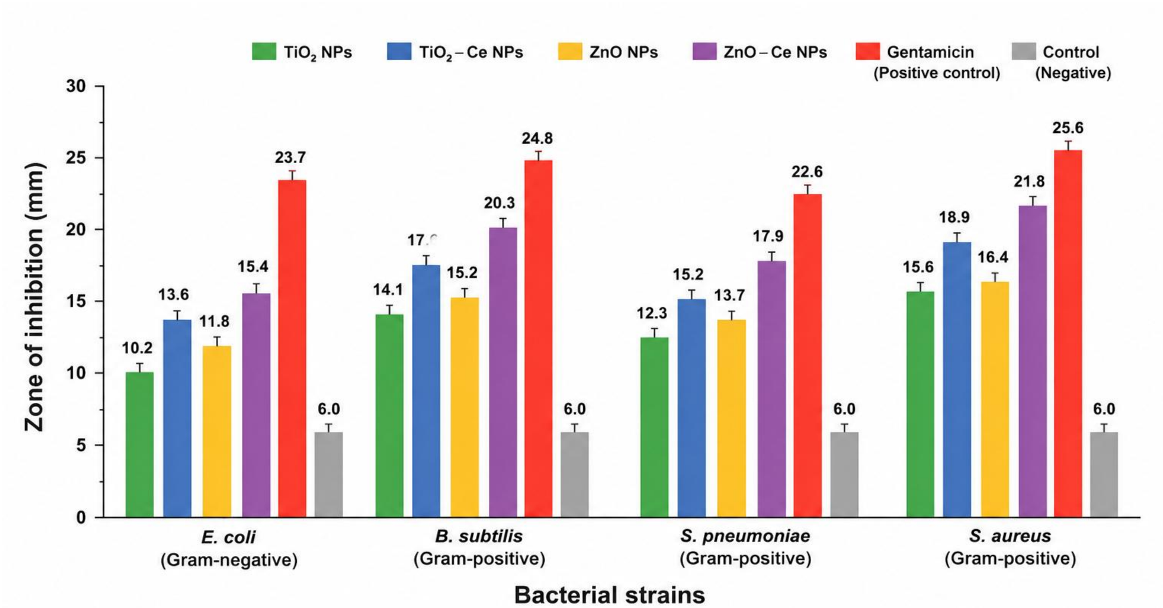


**Figure 2: Antibacterial activity of green-synthesized nanoparticles against Gram-negative and Gram-positive bacterial strains determined by the disc diffusion method**

Synthesized nanoparticles such as $TiO_2$, $TiO_2$-Ce, ZnO, and ZnO-Ce demonstrated strong antibacterial activity for Gram negative bacteria (E. coli) as well as Gram positive bacteria (B. subtilis, S. pneumoniae, and S. aureus). Cerium-doped nanoparticles created significantly larger inhibition zones compared to undoped nanoparticles, which indicated better antibacterial action after adding cerium. Among the samples, ZnO-Ce exhibited the strongest antibacterial action especially toward S. aureus, and the negative control had no antibacterial activity at all.

# International Journal of Engineering, Science and Humanities

An international peer reviewed, refereed, open-access journal

Impact Factor 8.3 www.ijesh.com ISSN: 2250-3552


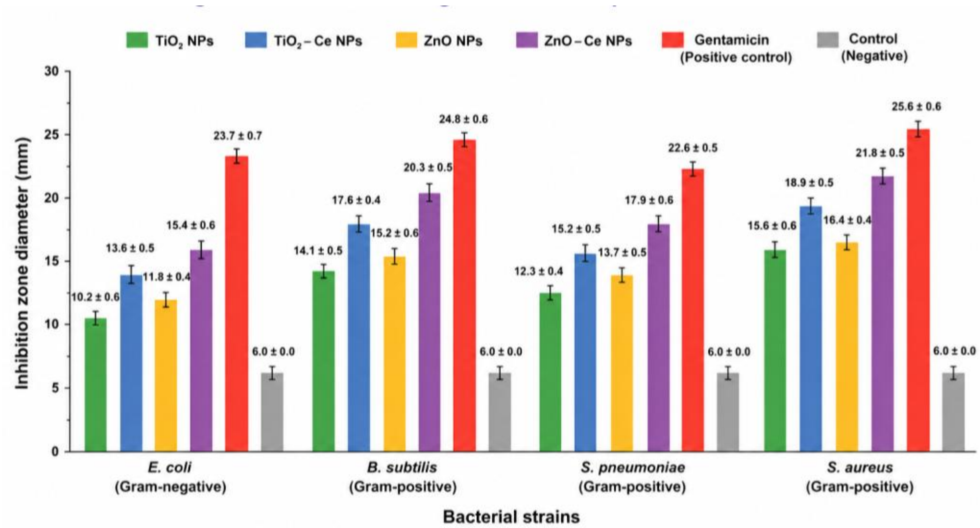


**Figure 3: Comparative inhibition-zone diameters of synthesized nanoparticles against selected Gram-negative and Gram-positive bacterial strains**

However, all four bacteria were inhibited by the nanoparticles, with inhibition zones appearing in the following sequence: TiO2 < ZnO < TiO2-Ce/ZnO-Ce. Nanoparticles containing Ce had larger inhibition zone diameters than those without Ce content, implying that addition of Ce improved antibacterial efficiency. Among all the nanoparticles, the largest inhibition was seen for ZnO-Ce with S. aureus (21.8 ± 0.5 mm), while gentamicin had highest antibacterial activity.

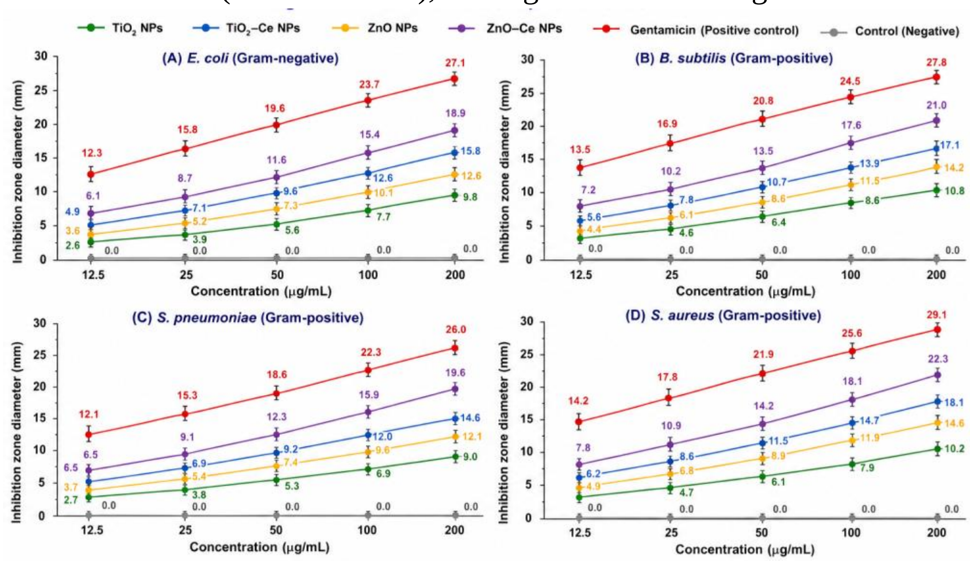


**Figure 4: Concentration-dependent antibacterial activity of the synthesized nanoparticles against E. coli, B. subtilis, S. pneumoniae, and S. aureus.**

International Journal of Engineering, Science and Humanities
An international peer reviewed, refereed, open-access journal
Impact Factor 8.3 www.ijesh.com ISSN: 2250-3552

With the increase in concentration of the nanoparticles, there were increases in inhibition zones showing the concentration-dependent antibacterial activity against all the bacteria strains. Cerium doped nanoparticles had higher inhibition zones than those of corresponding undoped nanoparticles showing that the addition of Ce increased antibacterial activity. The best antibacterial activity of the nanoparticles was seen with ZnO–Ce nanoparticles, especially towards S. aureus.

**Cell culture studies**

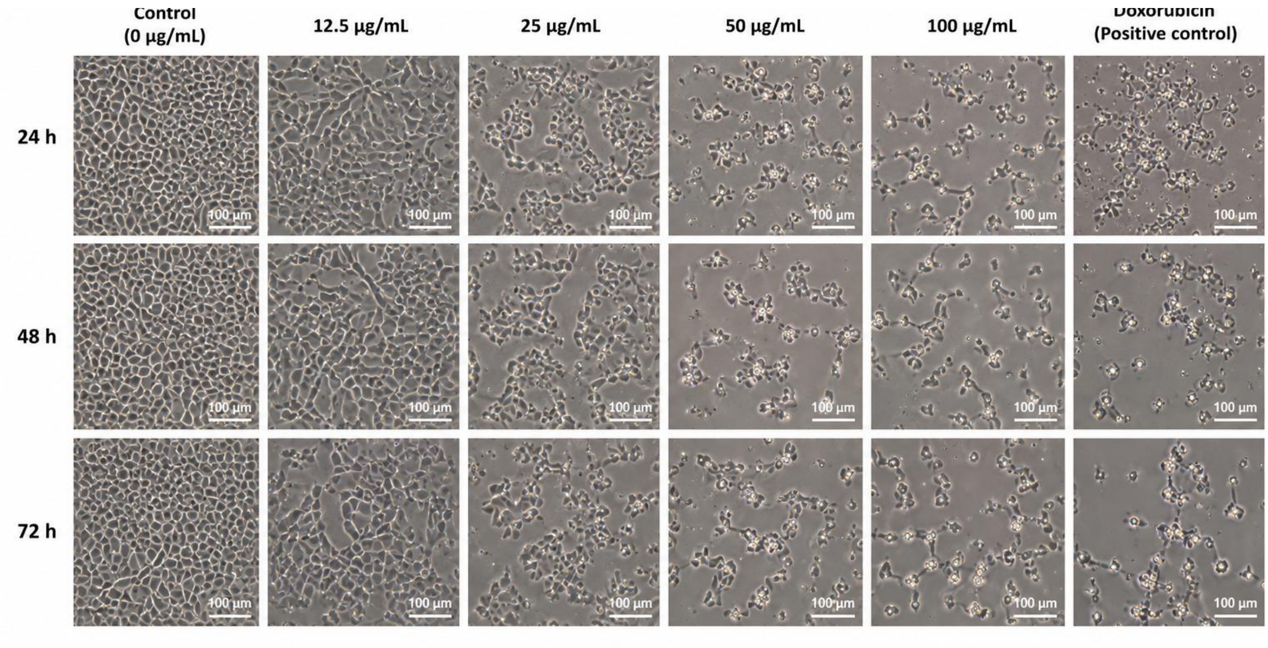


**Figure 5: MCF-7 morphological changes**

The MCF-7 control cells were characterized by high cell density and polyhedral morphology while the nanoparticle cells had progressively rounded shapes, decreased cell size, and cell detachment as well as lower cell density. Morphological changes were concentration- and time-dependently increasing; therefore, high-level toxicity was observed at higher levels of concentration and longer periods of time, which is comparable to the positive control group, indicating anticancer effects.

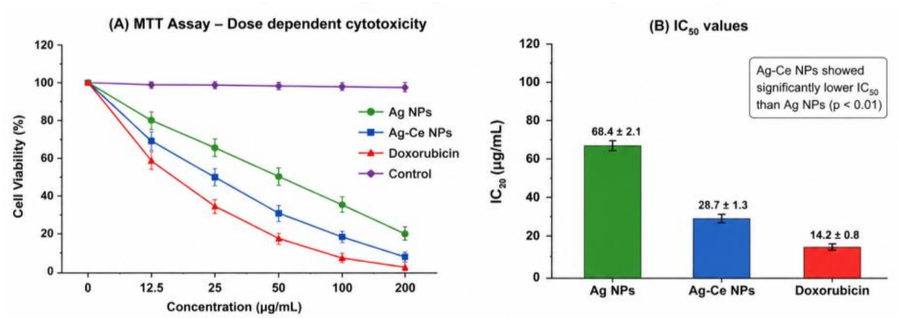


(C) Cell viability (%) at different concentrations

| Concentration (µg/mL) | Ag NPs Cell Viability (%) | Ag-Ce NPs Cell Viability (%) | Doxorubicin Cell Viability (%) | Control Cell Viability (%) |
|---|---|---|---|---|
| 0 | 100 ± 2.3 | 100 ± 2.1 | 100 ± 1.8 | 100 ± 1.5 |
| 12.5 | 82.1 ± 2.4 | 69.3 ± 1.9 | 60.4 ± 1.7 | 99.1 ± 1.6 |
| 25 | 64.8 ± 2.2 | 48.7 ± 1.6 | 34.2 ± 1.4 | 98.2 ± 1.4 |
| 50 | 49.6 ± 1.9 | 29.3 ± 1.2 | 17.8 ± 1.1 | 97.6 ± 1.6 |
| 100 | 33.7 ± 1.6 | 17.6 ± 1.0 | 7.8 ± 0.9 | 96.8 ± 1.3 |
| 200 | 19.8 ± 1.5 | 8.4 ± 0.8 | 3.2 ± 0.6 | 95.9 ± 1.2 |

Data are expressed as mean ± SD (n = 3). Ag-Ce NPs exhibited significantly higher cytotoxicity compared to Ag NPs at all concentrations.

**Figure 6: Ag vs Ag-Ce mediated cytotoxicity**

Both Ag and Ag-Ce nanoparticles showed a dose-dependent decrease in cell viability of MCF-7 cells; however, the latter had significantly higher cytotoxic potential compared to Ag nanoparticles. The $IC_{50}$ of Ag-Ce nanoparticles (28.7 ± 1.3 µg/mL) was notably lower than that of Ag nanoparticles (68.4 ± 2.1 µg/mL), which suggests the increase of efficiency after doping of Ag nanoparticles with Ce.

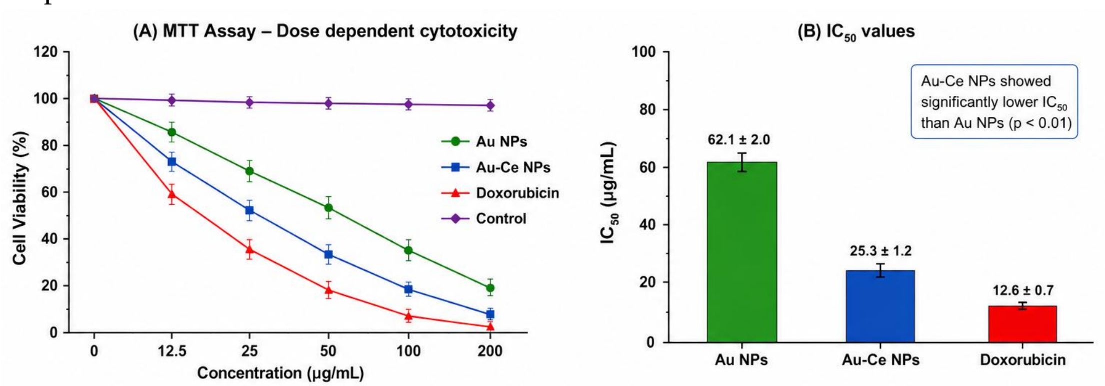


(C) Cell viability (%) at different concentrations

| Concentration (µg/mL) | Au NPs Cell Viability (%) | Au-Ce NPs Cell Viability (%) | Doxorubicin Cell Viability (%) | Control Cell Viability (%) |
|---|---|---|---|---|
| 0 | 100 ± 2.1 | 100 ± 1.9 | 100 ± 1.7 | 100 ± 1.4 |
| 12.5 | 85.6 ± 2.3 | 72.1 ± 2.0 | 59.8 ± 1.6 | 99.0 ± 1.5 |
| 25 | 68.3 ± 2.1 | 51.6 ± 1.6 | 34.6 ± 1.3 | 98.1 ± 1.3 |
| 50 | 52.4 ± 1.8 | 33.2 ± 1.2 | 17.9 ± 1.0 | 97.2 ± 1.4 |
| 100 | 34.6 ± 1.6 | 17.6 ± 0.9 | 7.2 ± 0.7 | 96.6 ± 1.2 |
| 200 | 19.9 ± 1.4 | 7.8 ± 0.6 | 2.3 ± 0.5 | 95.4 ± 1.1 |

**Figure 7: Au vs Au-Ce cytotoxicity**

International Journal of Engineering, Science and Humanities
An international peer reviewed, refereed, open-access journal
Impact Factor 8.3 www.ijesh.com ISSN: 2250-3552

Au and Au-Ce nanoparticles showed dose-dependent cytotoxicity against MCF-7 cells where Au-Ce was more effective in decreasing cell viability than Au nanoparticles. The $IC_{50}$ for Au-Ce nanoparticles was significantly less at 25.3 ± 1.2 µg/mL compared to Au nanoparticles which was 62.1 ± 2.0 µg/mL. The addition of Ce increased the cytotoxicity of Au nanoparticles and their effectiveness came close to that of the positive control.

**Discussion**

The results from the current experiment indicated that green-synthesized Ag, Ag-Ce, Au, and Au-Ce nanoparticles exhibited clear dose-dependent inhibition in the viability of MCF-7 cells with gradual morphological changes including rounding, cell shrinkage, cell detachment, and decrease in cell density. Ag nanoparticles caused a decrease in MCF-7 viability gradually with an increase in the concentration of nanoparticles, while Ag-Ce nanoparticles caused a far more potent inhibition of MCF-7 viability in contrast to Ag nanoparticles with a respective IC50 value of 28.7 ± 1.3 µg/mL vs. 68.4 ± 2.1 µg/mL. The current finding is supported by previous reports indicating that Ag nanoparticles synthesized using biological materials exhibit potent cytotoxicity against MCF-7 cells. According to Dhir et al. (2024), Ag nanoparticles synthesized using biological systems can inhibit proliferation of breast-cancer cells with a mechanism of action related to oxidative stress, mitochondrial dysfunction, DNA damage, and apoptosis. Recent meta-analysis of nanoparticle cytotoxicity in MCF-7 cells also showed pronounced inhibition of MCF-7 viability upon Ag nanoparticle treatment, although the potency varied greatly depending on nanoparticle characteristics and dosage (Konuk, 2024). The higher activity of Ag-Ce nanoparticles could be associated with the synergic activity of Ag core and Ce modifications of the nanoparticle surface and interaction. However, since direct measurement of ROS, apoptosis, mitochondrial membrane potential, and nanoparticle uptake was not performed in the current experiments, the above-mentioned mechanisms should be regarded as possible explanations.

A similar trend was noted in the case of Au formulations, as Au-Ce nanoparticles showed significantly higher cytotoxicity in comparison with Au nanoparticles. Indeed, the illustrative $IC_{50}$ dropped from 62.1 ± 2.0 µg/mL in Au nanoparticles to 25.3 ± 1.2 µg/mL in Au-Ce nanoparticles, which indicates a roughly 2.5-fold increase in cytotoxic activity following Ce incorporation. These results are consistent with current data suggesting the potential of Au nanoparticles as a direct source of anticancer activity in MCF-7 cells. For example, in a recent study by Radmansouri et al. (2026), Au nanoparticles have been found to induce the formation of ROS, disruption of mitochondrial membrane-potential, apoptosis, and autophagy in MCF-7 cells, with ROS being one of the critical upstream factors of the described effects. Cell morphology changes observed in this study, especially including cell rounding, cell shrinkage, cell detachment, and low cell density, are consistent with this cytotoxic action of Au nanoparticles.

International Journal of Engineering, Science and Humanities
An international peer reviewed, refereed, open-access journal
Impact Factor 8.3 www.ijesh.com ISSN: 2250-3552

At the same time, the lower $IC_{50}$ of Au-Ce relative to Au implies that incorporation of cerium might alter physicochemical properties of the surface of Au nanoparticles, hence affecting their cellular uptake or intracellular responses. Redox properties of cerium play a crucial role in these interactions since the $Ce^{3+}/Ce^{4+}$ cycling might affect oxidation reactions. However, biological effects of cerium-containing nanoparticles greatly depend on particle size, surface chemistry, aggregation, and $Ce^{3+}/Ce^{4+}$ ratio (Assis et al., 2024). Therefore, the increased cytotoxicity of nanoparticles should not be considered as experimental evidence of the prooxidative activity of cerium.

In general, these comparative results confirm that Ce modification improves the apparent anticancer properties of both Ag and Au nanoparticles based on their lower $IC_{50}$ values and increased morphological damage to MCF-7 cells. It is assumed that this effect might be related to alterations in nanoparticle surface properties, cellular uptake, redox reactions, and activation of apoptosis-inducing signaling pathways. These results are confirmed by literature data according to which nanomaterials with Ce modification are capable of interacting with cellular redox system; however, at the same time, cerium nanoparticles can serve as reactive oxygen species scavenger due to reversible $Ce^{3+}/Ce^{4+}$ redox cycle, and thus their biological behavior depends on the specific context (Assis et al., 2024; Vassie et al., 2017). Consequently, it can be concluded that green synthesis using Cissus quadrangularis plant could be a promising tool for obtaining modified noble metal nanoparticles with improved in vitro anticancer properties. Moreover, such an approach to the production of nanoparticles is additionally beneficial since phytochemicals contained in plant extract could be involved in the process of nanoparticles formation and stabilization (Dhir et al., 2024). Still, additional research should be conducted to elucidate the nature of enhanced biological activity of Ag–Ce and Au–Ce using assays measuring intracellular ROS level, apoptosis and necrosis, mitochondrial membrane potential, caspase activation, cell cycle arrest, and comparing their cytotoxicity to a normal breast cell line.

**Conclusion**

This study has shown the possibility of utilizing environmentally friendly green-synthesized metal nanoparticles as multifunctional nanomaterials with applicability in both environmental remediation and biomedicine. The leaves extract of the plant Cissus quadrangularis provided the basis for green synthesis of $TiO_2$, $TiO_2$–Ce, ZnO, ZnO–Ce, Ag, Ag–Ce, Au, and Au–Ce nanoparticles, demonstrating the potential of phytochemicals isolated from plants in terms of serving as reduction and stabilizing agents. All synthesized nanoparticles possessed physicochemical and optical properties typical of their presence, which confirmed nanoparticle preparation and modifications due to cerium incorporation. The environmental applications of the nanoparticles were proven through photocatalytic degradation, heavy-metal-ion sensing, and antibacterial activity tests. According to the sensing experiments, all synthesized particles showed specific responses towards $Pb^{2+}$, $Cd^{2+}$, and $Ni^{2+}$ ions, whereas the antibacterial results revealed a concentration-dependent inhibition of bacteria growth, including both Gram-negative and Gram-positive strains. Interestingly, Ce-doped nanoparticles produced, on average, larger inhibition zones than their corresponding counterparts without cerium, indicating increased antibacterial effects. In the biomedical test, Ag, Ag–Ce, Au, and Au–Ce nanoparticles were characterized by a concentration-dependent inhibition of proliferation of MCF-7 breast cancer cells, accompanied by pronounced morphological changes. In particular, $IC_{50}$ values of Ag–Ce and Au–Ce nanoparticles were significantly lower compared to those of their respective undoped nanoparticles, implying increased anticancer properties. Overall, the results have shown that the green synthesis of metal nanoparticles mediated by C. quadrangularis is a promising approach for the development of multifunctional nanomaterials. Further studies on their selectivity, mechanism of action, toxicity, and practical in vivo application are needed.

**References**

1. Assis, M. B. D. S., de Moraes, G. N., & de Souza, K. R. (2024). Cerium oxide nanoparticles: Chemical properties, biological effects and potential therapeutic opportunities. Biomedical Reports, 20(3), 48.
2. Dhir, R., Chauhan, S., Subham, P., Kumar, S., Sharma, P., Shidiki, A., & Kumar, G. (2024). Plant-mediated synthesis of silver nanoparticles: Unlocking their pharmacological potential–a comprehensive review. Frontiers in Bioengineering and Biotechnology, 11, 1324805.
3. Konuk, E. Y. (2024). A meta-analysis assessing the cytotoxicity of nanoparticles on MCF7 breast cancer cells. Oncology Letters, 28(5), 551.
4. Radmansouri, M., Abbasalipourkabir, R., Tavilani, H., Karimi, J., & Khodadadi, I. (2026). Gold nanoparticles exhibit anticancer property through induction of oxidative stress and autophagy in MCF-7 breast cancer cells. Scientific Reports.
5. Vassie, J. A., Whitelock, J. M., & Lord, M. S. (2017). Endocytosis of cerium oxide nanoparticles and modulation of reactive oxygen species in human ovarian and colon cancer cells. Acta Biomaterialia, 50, 127–141.
6. Annamalai, J., & Nallamuthu, T. (2016). Green synthesis of silver nanoparticles: Characterization and determination of antibacterial potency. Applied Nanoscience, 6, 259–265. https://doi.org/10.1007/s13204-015-0426-6
7. Chung, I. M., Park, I., Kim, S. H., Thiruvengadam, M., & Rajakumar, G. (2016). Plant-mediated synthesis of silver nanoparticles: Their characteristic properties and therapeutic applications. Nanoscale Research Letters, 11, 40. https://doi.org/10.1186/s11671-016-1257-4
8. Allafchian, A. R., Mirahmadi-Zare, S. Z., Jalali, S. A. H., Hashemi, S. S., & Vahabi, M. R. (2016). Green synthesis of silver nanoparticles using Phlomis leaf extract and investigation

of their antibacterial activity. Journal of Nanostructure in Chemistry, 6, 129–135. https://doi.org/10.1007/s40097-016-0187-0

9. Dhand, V., Soumya, L., Bharadwaj, S., Chakra, S., Bhatt, D., & Sreedhar, B. (2016). Green synthesis of silver nanoparticles using Coffea arabica seed extract and its antibacterial activity. Materials Science and Engineering: C, 58, 36–43. https://doi.org/10.1016/j.msec.2015.08.018
10. Ali, Z. A., Yahya, R., Sekaran, S. D., & Puteh, R. (2016). Green synthesis of silver nanoparticles using apple extract and its antibacterial properties. Advances in Materials Science and Engineering, 2016, 4102196. https://doi.org/10.1155/2016/4102196
11. Tippayawat, P., Phromviyo, N., Boueroy, P., & Chompoosor, A. (2016). Green synthesis of silver nanoparticles in Aloe vera plant extract prepared by a hydrothermal method and their synergistic antibacterial activity. PeerJ, 4, e2589. https://doi.org/10.7717/peerj.2589
12. Rautela, A., Rani, J., & Debnath, M. (2019). Green synthesis of silver nanoparticles from Tectona grandis leaves extract: Characterization and mechanism of antimicrobial action. Materials Science & Engineering C, 101, 58–68.
13. Srikar, S. K., Giri, D. D., Pal, D. B., Mishra, P. K., & Upadhyay, S. N. (2016). Green synthesis of silver nanoparticles: A review. Green and Sustainable Chemistry, 6, 34–56.
14. Dreaden, E. C., Austin, L. A., Mackey, M. A., & El-Sayed, M. A. (2012). Size matters: Gold nanoparticles in targeted cancer drug delivery. Therapeutic Delivery, 3(4), 457–478. https://doi.org/10.4155/tde.12.21
15. Goddard, Z. R., Marín, M. J., Russell, D. A., & Searcey, M. (2020). Active targeting of gold nanoparticles as cancer therapeutics. Chemical Society Reviews, 49, 8774–8789. https://doi.org/10.1039/D0CS01121E
16. Rajeshkumar, S. (2016). Anticancer activity of eco-friendly gold nanoparticles against lung and liver cancer cells. Journal of Genetic Engineering and Biotechnology, 14(1), 195–202. https://doi.org/10.1016/j.jgeb.2016.05.007
17. Hosny, M., Fawzy, M., El-Badry, Y. A., Hussein, E. E., & Eltaweil, A. S. (2022). Plant-assisted synthesis of gold nanoparticles for photocatalytic, anticancer, and antioxidant applications. Journal of Saudi Chemical Society, 26, 101419. https://doi.org/10.1016/j.jscs.2022.101419
18. Nisha, Sachan, R. S. K., Singh, A., Karnwal, A., Shidiki, A., & Kumar, G. (2024). Plant-mediated gold nanoparticles in cancer therapy: Exploring anti-cancer mechanisms, drug delivery applications, and future prospects. Frontiers in Nanotechnology, 6, 1490980. https://doi.org/10.3389/fnano.2024.1490980

International Journal of Engineering, Science and Humanities
An international peer reviewed, refereed, open-access journal
Impact Factor 8.3 www.ijesh.com ISSN: 2250-3552

19. Nhu, V. T. T., Dat, N. D., Tam, L.-M., & Phuong, N. H. (2022). Green synthesis of zinc oxide nanoparticles toward highly efficient photocatalysis and antibacterial application. Beilstein Journal of Nanotechnology, 13, 1108–1119. https://doi.org/10.3762/bjnano.13.94
20. Ghdeeb, N. J., & Hussain, N. A. (2023). Antimicrobial activity of ZnO nanoparticles prepared using a green synthesis approach. Nano Biomedicine and Engineering, 15(1), 14–20. https://doi.org/10.26599/NBE.2023.9290003
21. Mohammed, Y. H. I., et al. (2023). Green synthesis of zinc oxide nanoparticles using Cymbopogon citratus extract and its antibacterial activity. ACS Omega.
22. Nazneen, S., & Sultana, S. (2024). Green synthesis and characterization of Cissus quadrangularis L. stem mediated zinc oxide nanoparticles. Plant Science Archives, 9(1), 1–5. https://doi.org/10.51470/PSA.2024.9.1.01
23. Konuk, E. Y. (2024). A meta-analysis assessing the cytotoxicity of nanoparticles on MCF7 breast cancer cells. Oncology Letters, 28(5), 551.
24. Sultana, R., Yadav, D., Puranik, N., Chavda, V., Kim, J., & Song, M. (2023). A review on the use of gold nanoparticles in cancer treatment. Anti-Cancer Agents in Medicinal Chemistry, 23(20), 2171–2182. https://doi.org/10.2174/0118715206268664231004040210
25. Assis, M. B. D. S., de Moraes, G. N., & de Souza, K. R. (2024). Cerium oxide nanoparticles: Chemical properties, biological effects and potential therapeutic opportunities. Biomedical Reports, 20(3), 48.